

# ON-DEVICE FINE-TUNING VIA BACKPROP-FREE ZERO-TH-ORDER OPTIMIZATION

Prabodh Katti, Sangwoo Park, Bipin Rajendran, and Osvaldo Simeone

CIIPS, Department of Engineering, King’s College London

## ABSTRACT

On-device fine-tuning is a critical capability for edge AI systems, which must support adaptation to different agentic tasks under stringent memory constraints. Conventional backpropagation (BP)-based training requires storing layer activations and optimizer states, a demand that can be only partially alleviated through checkpointing. In edge deployments in which the model weights must reside entirely in device memory, this overhead severely limits the maximum model size that can be deployed. Memory-efficient zeroth-order optimization (MeZO) alleviates this bottleneck by estimating gradients using forward evaluations alone, eliminating the need for storing intermediate activations or optimizer states. This enables significantly larger models to fit within on-chip memory, albeit at the cost of potentially longer fine-tuning wall-clock time. This paper first provides a theoretical estimate of the relative model sizes that can be accommodated under BP and MeZO training. We then numerically validate the analysis, demonstrating that MeZO exhibits accuracy advantages under on-device memory constraints, provided sufficient wall-clock time is available for fine-tuning.

**Keywords:** LLM, Fine-Tuning, MeZO.

## 1. INTRODUCTION

**Context and Motivation:** A key avenue for advancing artificial intelligence (AI) performance is tailoring models to specific tasks and user needs via fine-tuning [1], particularly for agentic systems [2]. User demands for modern AI models are not static, making fine-tuning a recurring necessity rather than a one-time cost. On-device fine-tuning directly addresses this need, enabling edge devices to adapt models without relying on external servers.

However, fine-tuning may be substantially more memory-intensive than inference. In edge deployments, the model must ideally fit in the device memory [3, 4], a requirement that is potentially well aligned with recent calls for small language models as the engine of agentic AI [5]. However, in order to enable fine-tuning, one is forced to implement smaller-scale models as compared to inference-only settings. This paper examines a possible solution to this problem, moving away from conventional backpropagation (BP) towards

This project is funded by the Advanced Research + Invention Agency (ARIA).

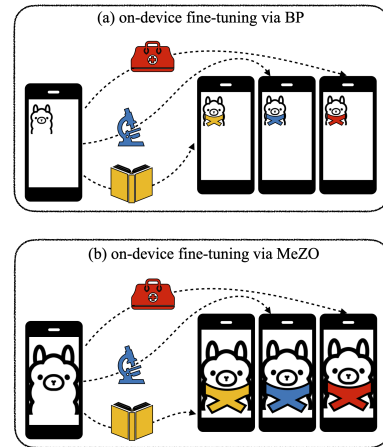


**Fig. 1.** On-device fine-tuning: (a) backpropagation (BP)-based fine-tuning requires significantly more memory than inference (see Fig. 3), limiting model size on the device; while (b) MeZO-based fine-tuning [6] only carries out inference steps, enabling deployment of significantly larger, more capable models at the edge.

memory-efficient zeroth-order optimization (MeZO) [6]. An experimental demonstration of MeZO on edge devices was described in [7].

BP incurs a heavy memory overhead because it requires storing intermediate activations for every layer, resulting in memory demands far exceeding those of inference [8, 6]. Even with techniques such as activation checkpointing [9], BP often remains impractical for resource-constrained devices. For instance, fine-tuning a 13B-parameter transformer can require an order-of-magnitude more memory than a single forward pass, implying that even an 80 GB GPU can only accommodate models on the order of 3 billion parameters using BP [6].

In contrast, MeZO provides a memory-efficient alternative by estimating gradients through function evaluations rather than explicit derivatives. A classical approach rooted in simultaneous perturbation stochastic approximation (SPSA) [10], MeZO approximates gradients using only forward passes. While this eliminates the need to store intermediate activations, MeZO’s convergence rates degrade with the size of the parameter vector [11]. Recent advances, however, have shown that strong pre-training substantially reduces the effective di-

mensionality of the parameter space to be updated, making MeZO surprisingly competitive for fine-tuning [6].

Since the initial demonstration in [6], researchers have developed several extensions of MeZO. For example, Sparse MeZO updates only a subset of parameters at each step [12], AdaZeta combines MeZO with parameter-efficient fine-tuning [13], and LoHo integrates occasional BP-based gradient updates [14].

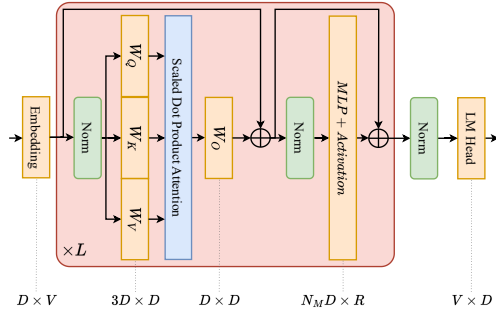


**Fig. 2.** Illustration of a basic decoder-only Transformer model, highlighting the major contributors to parameter count. Non-parametric operations such as RoPE encoding [15] and parameter count for minor contributors, such as normalization layers, are not shown for clarity.

**Main Contributions:** This paper provides a comprehensive study of on-device fine-tuning for LLMs, comparing BP and MeZO approaches. Our main contributions are:

- **Memory analysis of BP vs. MeZO:** We derive theoretical limits on model sizes that can be fine-tuned under fixed on-chip memory budgets, showing that MeZO can accommodate models at least  $2\times$  larger than BP within the same budget. This advantage grows with longer context windows, reaching up to  $25\times$  as the context length increases (see Fig. 3).
- **Empirical evaluation:** We numerically validate the analysis, demonstrating that MeZO exhibits accuracy advantages under on-device memory constraints, provided sufficient wall-clock time is available for fine-tuning.

## 2. MEMORY REQUIREMENTS OF BP AND MEZO

In this section, we analyze the memory requirements of BP and ZO-based fine-tuning for Transformer models with the aim of providing theoretical limits on the model size that can be accommodated under a fixed on-chip memory budget.

Throughout this section, as illustrated in Fig. 2, we focus on a basic decoder-only Transformer architecture, using the notation summarized in Table 1. Specifically, we concentrate on traditional multi-head global self-attention and single-expert feedforward neural networks (FFN). These choices exclude the use of sliding-window attention [16] and mixture-of-experts architectures [17, 18]. However, the analysis reported in this section can be generalized to these modern architectural vari-

**Table 1.** Notations used in text

Symbol	Definition
$N$	Context length
$L$	Number of layers
$D$	Hidden dimension
$H$	Number of attention heads
$K$	Key/ value heads ( $=H$ assumed here)
$N_M$	Number of MLPs in FFN layer
$R$	MLP expansion factor (hidden size $D \times R$ )
$V$	Vocabulary size
$B$	Batch size
$b$	Bytes per parameter

ants by introducing variables such as window-size and expert count, without affecting the general conclusions.

### 2.1. Parameter Count

In order to establish the memory footprints of BP and MeZO, we start by counting the number of model parameters. For decoder-only LLMs, the model is largely composed of multi-head attention blocks and FFN layers, along with embedding layers and language model (LM) head.

- **Multi-head attention:** Given the embedding dimension  $D$ , the parameters per attention head encompass four projection matrices, typically denoted as  $W_Q, W_K, W_V, W_O$ , each of dimension  $D \times D$ . This yields a total of  $4D^2$  parameters per layer.
- **Feedforward neural networks:** Given an expansion factor  $R$  between the embedding dimension and the FFN hidden dimension, the number of parameters per FFN layer is proportional to the product  $DR$ . In models such as LLaMa-2 and GPT-2, the value of  $R$  is proportional to  $D$ , e.g.,  $R \approx 2.67D$  for Llama-2 and  $R = 4D$  for GPT-2. Therefore the total number of parameters is proportional to  $D^2$ . The total parameter count for both models is approximated as  $N_M L D R$ . For GPT-2 and LLaMa-2, substituting the values of  $\{N_M = 2, R = 4D\}$  and  $\{N_M = 3, R = 2.67D\}$  respectively, we obtain the total parameter count for FFN layers as  $8LD^2$  for both models [19][20].
- **Embedding layers, language model head, and normalizing layers:** Both the embedding layer and the LM head have  $VD$  parameters. This makes them bigger than projection matrices or MLPs in FFN. However, their contributions do not scale with the number of layers  $L$ , since they are not repeated at each layer. Normalizing layers such as RMSNorm or LayerNorm have parameter counts proportional to  $D$ , so they only contribute a negligible fraction to the total parameter count.

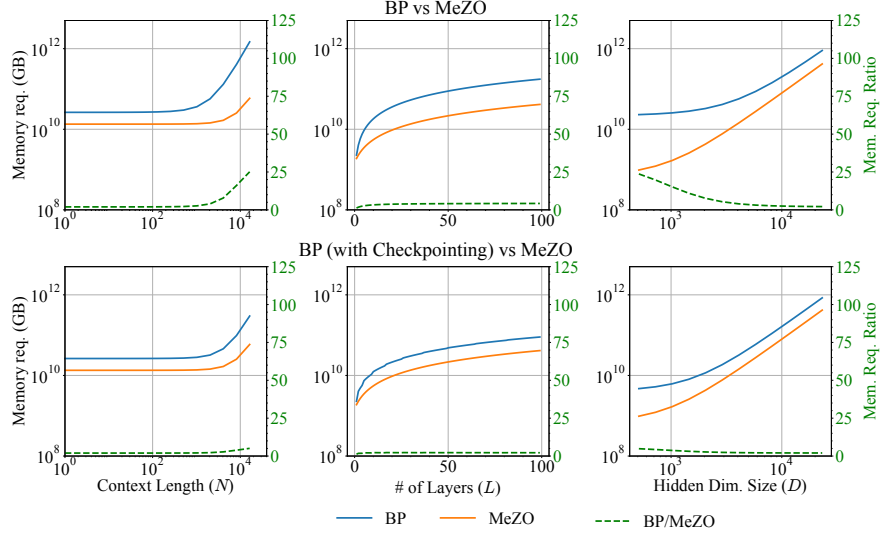


**Fig. 3.** Memory requirements for BP- and MeZO-based fine-tuning, including conventional BP (top row) and BP with checkpointing (bottom row). The solid lines and the primary y-axis correspond to the total memory consumed by BP and MeZO using (2), while the secondary y-axis with a green colored dashed line represents the MeZO over BP ratio of memory requirements.

Based on this analysis, we approximate the total parameter count as  $4D^2 + 8D^2 + 2VD = 12D^2 + 2VD$ .

## 2.2. Activation Count

With BP, activations must be cached for all layers. As detailed in [8], the total memory of activation elements in bytes is approximately

$$A = BLND \left( 2 + 16b + \frac{(2b+1)NH}{D} \right), \quad (1)$$

where  $b$  is the number of bytes per parameter.

In contrast, MeZO does not require intermediate activation storage, as it only operates based on forward passes.

## 2.3. Total Memory

Assuming a stateless SGD optimizer, summing the contributions of model parameters and activations, the total memory requirement for BP can be estimated as

$$M_{BP} = 24bLD^2 + 4bVD + A, \quad (2)$$

encompassing the contributions of model weights ( $12bLD^2$ ), gradients ( $12bLD^2$ ), the embedding layer, the LM head and corresponding gradients ( $bVD$  each), and activations using (1). With activation checkpointing, one can replace the number of layers  $L$  in (1) with a smaller number, typically  $\sqrt{L}$ , as the remaining activations are recomputed as needed [9].

Since MeZO stores no activations and does not involve gradient computation, the memory is in principle dominated

by parameters. In practice, however, the memory requirements depend on memory allocation and management policies, controlling the buffering of intermediate tensors [21]. To account for this implementation-specific aspect, we introduce a factor  $L' \leq L$ , which dictates the maximum number of layers of activations stored by MeZO. This yields the memory requirement

$$M_{MeZO} = 12bLD^2 + 2bVD + \frac{L'}{L}A. \quad (3)$$

## 2.4. Numerical Example

Fig. 3 illustrates the memory requirements of BP, both with and without checkpointing (first and second row, respectively), and MeZO, along with the corresponding ratio between the memory requirements of BP and MeZO, when we vary context length  $N$  (first column), number of layers  $L$  (second column), and hidden dimension size  $D$  (third column). For BP with activation checkpointing, following [9], we assume the storage of activations for only  $\sqrt{L}$  layers. We adopt the LLaMa-2 7B model, for which the relevant variables in Table 1 are set as  $B = 1$ ,  $V = 32000$ ,  $N = 2048$ ,  $L = 32$ ,  $b = 2$  (FP16),  $H = 32$ , and  $D = 4096$ . For the first column in Fig. 3, the context length  $N$  was varied from 1 to 32768, with  $D$  and  $L$  fixed to their default values; while for the second and third columns the parameter  $L$  was varied from 1 to 100 and  $D$  from 512 to 32768, while keeping parameters  $(N, D)$  and  $(N, L)$  fixed respectively. The dynamic memory allocation parameter  $L'$  for MeZO was set to 1.

**Context scaling:** The top-left panel of Fig. 3 describes the memory requirements with increasing context size for BP

without checkpointing and for MeZO. The activation memory increase is quadratic with context, with BP memory requirement growth outpacing MeZO as per (2) and (3). As a result, the memory savings afforded by MeZO range from  $2\times$  at moderate contexts to up to  $25\times$  for  $N = 32768$ . As seen in the bottom-left part of Fig 3. with activation checkpointing, the advantage of MeZO over BP reduces to approximately  $5\times$  for long contexts, while remaining unchanged for smaller ones.

**Layer scaling:** Parameter memory scales linearly with  $L$  for both BP and MeZO. The top and bottom center panels in Fig. 3 show that for BP without checkpointing, the gain afforded by BP is smaller, around  $1.2\times$ , when  $L$  is small due to the contributions from the embedding layer and the LM head. These contributions diminish with larger  $L$ , and the memory savings increases to  $4.23\times$  for larger  $L$ , with an asymptotic limit of 4.38. The effect of checkpointing on the MeZO/BP memory ratio is more significant for large layer sizes  $L$ . Specifically, the peak gain of around  $2.28\times$  at lower  $L$  reduces slowly to  $2.17\times$  for  $L = 100$ , approaching the asymptotic gain of  $2\times$ .

**Hidden dimension scaling:** The dependence of parameter count with the hidden dimension  $D$  is quadratic (see (2) and (3)). As shown in the right column of Fig. 3, this results in a rapid increase in memory for both BP and MeZO. For smaller  $D$ , the memory saving of MeZO can be as high as approximately  $24\times$ , which reduces to  $5\times$  with BP checkpointing. With larger  $D$ , the memory saving ratio converges to 2.

Based on this analysis, we can conclude that, for the same memory budget, we can fine-tune a model that is at least  $2\times$  larger when using MeZO as compared to using BP, with potentially several orders-of-magnitude larger savings for large contexts.

### 3. EXPERIMENTS

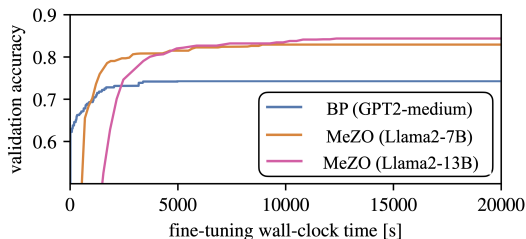


**Fig. 4.** On-device fine-tuning for Boolq data set [22] as a function of fine-tuning wall-clock time [s]. We consider MeZO with Llama2-7B and LLaMa2-13B, while BP adopts GPT2-medium model. The batch size is  $B = 8$ . All models require a similar memory consumption of around 17 GB according to the analysis in Sec. 2 when setting  $L'/L = 0.15$  for Llama2-13B and the  $L'/L = 0.41$  for Llama2-7B.

This section validates the main claim of this work that MeZO can support the deployment of more powerful edge

AI models when fine-tuning must be implemented on the device. We adopt the Boolq data set [22] with the prompting technique in [23] to support binary question answering. All the experiments are carried out using a single H100 GPU.

From the analysis in Sec. 2, under the maximum context length  $N = 1024$  with batch size  $B = 8$ , fine-tuning GPT2-medium using BP has a memory requirement of around 17 GB. We consider two different settings in terms of the implementation-specific parameter  $L'$  in (3) for MeZO. Recall that a maximally efficient implementation corresponds to  $L'/L = 0$ , while the BP memory requirement is recovered with  $L'/L = 1$ . We evaluate two intermediate cases, namely  $L'/L = 0.15$  and  $L'/L = 0.41$ . Using (3), a memory of around 17GB is obtained with MeZO when fine-tuning Llama2-7B if  $L'/L = 0.41$  and Llama2-13B if  $L'/L = 0.15$ .

In Fig. 4, we show the validation accuracy as a function of fine-tuning wall-clock time. We report the running maximum value for the accuracy. We use vanilla SGD with fixed learning rate for both BP and MeZO with learning rate chosen by grid search. Specifically, we set the learning rate grid for BP as  $[5e-4, 5e-5, 5e-6]$  and for MeZO as  $[5e-7, 5e-8, 5e-9]$ , and report in Fig. 4 the highest accuracy for both schemes. We fix the number of perturbations for MeZO to 5 [6]. Note that the number of perturbations does not affect the memory requirements of MeZO.

Fig. 4 confirms that MeZO has a slower fine-tuning convergence rate in terms of wall-clock time. However, thanks to the more capable model afforded by its more efficient memory usage, MeZO can eventually achieve a higher validation accuracy. For example, after about 2 hours, the accuracy of MeZO is around 82%, while that of BP remains below 75%.

### 4. CONCLUSIONS

MeZO optimization eliminates the need to store activations and optimizer states, reducing training memory demands to the level of inference memory. This enables on-device learning with larger models and longer contexts. We have analyzed the relative memory requirements of MeZO compared to conventional BP-based fine-tuning and presented experimental results benchmarking their achievable accuracy on edge models. Overall, these findings position MeZO as a strong candidate for scenarios that require on-device fine-tuning, including agentic edge systems and neuromorphic architectures for continual learning. More research is required to specialize the main conclusions to neuromorphic systems and other models with dynamic sparsity at the level of activations.

### 5. REFERENCES

- [1] V. Lialin, V. Deshpande, and A. Rumshisky, “Scaling down to scale up: A guide to parameter-efficient fine-tuning,” *arXiv preprint arXiv:2303.15647*, 2023.

- [2] B. Chen, C. Shu, E. Shareghi, N. Collier, K. Narasimhan, and S. Yao, “Fireact: Toward language agent fine-tuning,” *arXiv preprint arXiv:2310.05915*, 2023.
- [3] G. Slamanig, F. Corti, and O. Saukh, “From llms to edge: Parameter-efficient fine-tuning on edge devices,” *arXiv preprint arXiv:2507.23536*, 2025.
- [4] R. Aralimatti, S. A. G. Shakhadri, K. R. Kruthika, and K. B. Angadi, “Fine-Tuning Small Language Models for Domain-Specific AI: An Edge AI Perspective,” in *Intelligent Systems and Applications*, K. Arai, Ed. Springer Nature Switzerland, 2025, pp. 503–520.
- [5] P. Belcak, G. Heinrich, S. Diao, Y. Fu, X. Dong, S. Muralidharan, Y. C. Lin, and P. Molchanov, “Small language models are the future of agentic ai,” *arXiv preprint arXiv:2506.02153*, 2025.
- [6] S. Malladi, T. Gao, E. Nichani, A. Damian, J. D. Lee, D. Chen, and S. Arora, “Fine-tuning language models with just forward passes,” *Advances in Neural Information Processing Systems*, vol. 36, pp. 53 038–53 075, 2023.
- [7] D. Peng, Z. Fu, and J. Wang, “PocketLLM: Enabling on-device fine-tuning for personalized LLMs,” in *Proceedings of the Fifth Workshop on Privacy in Natural Language Processing*. Bangkok, Thailand: Association for Computational Linguistics, Aug. 2024, pp. 91–96. [Online]. Available: <https://aclanthology.org/2024.privatenlp-1.10/>
- [8] V. A. Korthikanti, J. Casper, S. Lym, L. McAfee, M. Andersch, M. Shoeybi, and B. Catanzaro, “Reducing activation recomputation in large transformer models,” *Proceedings of Machine Learning and Systems*, vol. 5, pp. 341–353, 2023.
- [9] K. Panchal *et al.*, “The cost of avoiding backpropagation,” 2025, arXiv preprint. [Online]. Available: <https://arxiv.org/abs/2506.21833>
- [10] J. C. Spall, “An overview of the simultaneous perturbation method for efficient optimization,” *Johns Hopkins APL Technical Digest*, vol. 19, no. 4, pp. 482–492, 1998.
- [11] J. C. Duchi, M. I. Jordan, M. J. Wainwright, and A. Wibisono, “Optimal rates for zero-order convex optimization: The power of two function evaluations,” *IEEE Transactions on Information Theory*, vol. 61, no. 5, pp. 2788–2806, 2015.
- [12] Y. Liu, Z. Zhu, C. Gong, M. Cheng, C.-J. Hsieh, and Y. You, “Sparse MeZO: Less parameters for better performance in zeroth-order LLM fine-tuning,” in *International Conference on Machine Learning (ICML)*, 2024. [Online]. Available: <https://arxiv.org/abs/2402.11888>
- [13] Y. Yang, K. Zhen, E. Banijamali, A. Mouchtaris, and Z. Zhang, “AdaZeta: Adaptive zeroth-order tensor-train adaptation for memory-efficient large language model fine-tuning,” in *Empirical Methods in Natural Language Processing (EMNLP)*, 2024. [Online]. Available: <https://arxiv.org/abs/2406.08301>
- [14] M. Chen, Y.-L. Huang, and Z. Wen, “Towards efficient low-order hybrid optimizer for language model fine-tuning,” in *AAAI Conference on Artificial Intelligence*, 2025, preprint. [Online]. Available: <https://arxiv.org/abs/2409.18075>
- [15] J. Su, M. Ahmed, Y. Lu, S. Pan, W. Bo, and Y. Liu, “Roformer: Enhanced transformer with rotary position embedding,” *Neurocomput.*, vol. 568, no. C, Feb. 2024. [Online]. Available: <https://doi.org/10.1016/j.neucom.2023.127063>
- [16] I. Beltagy, M. E. Peters, and A. Cohan, “Longformer: The long-document transformer,” *arXiv preprint arXiv:2004.05150*, 2020.
- [17] N. Shazeer, A. Mirhoseini, K. Maziarz, A. Davis, Q. Le, G. Hinton, and J. Dean, “Outrageously large neural networks: The sparsely-gated mixture-of-experts layer,” in *International Conference on Learning Representations*, 2017. [Online]. Available: <https://openreview.net/forum?id=B1ckMDqIq>
- [18] R. A. Jacobs, M. I. Jordan, S. J. Nowlan, and G. E. Hinton, “Adaptive mixtures of local experts,” *Neural computation*, vol. 3, no. 1, pp. 79–87, 1991.
- [19] A. Radford, J. Wu, R. Child, D. Luan, D. Amodei, I. Sutskever *et al.*, “Language models are unsupervised multitask learners,” *OpenAI blog*, vol. 1, no. 8, p. 9, 2019.
- [20] H. Touvron, L. Martin, K. Stone, P. Albert, A. Almahairi, Y. Babaei, N. Bashlykov, S. Batra, P. Bhargava, S. Boschale *et al.*, “Llama 2: Open foundation and fine-tuned chat models,” *arXiv preprint arXiv:2307.09288*, 2023.
- [21] Z. Huang, J. Hu, H. Lin, C. Zhu, Y. Tang, Q. Zhang, Z. Guo, Z. Li, S. Yan, Z. Zhu *et al.*, “Reducing gpu memory fragmentation via spatio-temporal planning for efficient large-scale model training,” *arXiv preprint arXiv:2507.16274*, 2025.
- [22] C. Clark, K. Lee, M.-W. Chang, T. Kwiatkowski, M. Collins, and K. Toutanova, “Boolq: Exploring the surprising difficulty of natural yes/no questions,” in *NAACL*, 2019.
- [23] T. Gao, A. Fisch, and D. Chen, “Making pre-trained language models better few-shot learners,” *arXiv preprint arXiv:2012.15723*, 2020.